Available online at http://scik.org
Commun. Math. Biol. Neurosci. 2023, 2023:25
https://doi.org/10.28919/cmbn/7825
ISSN: 2052-2541

EFFECT OF PARTIALLY AND FULLY VACCINATED INDIVIDUALS IN SOME REGIONS OF INDIA: A MATHEMATICAL STUDY ON COVID-19 OUTBREAK

M. AAKASH, C. GUNASUNDARI*

Department of Mathematics, SRM Institute of Science and Technology, Chengalpattu 603203, India

Abstract. In this paper, we investigate the effect of partially vaccinated and fully vaccinated individuals in preventing the transmit of COVID-19, especially in the regions of Tamil Nadu, Maharashtra, West Bengal and Delhi. Here we construct an *SEIR* model and analyse the behaviour. We obtained R_0 by using next generation matrix approach. Also, our system shows two types of equilibria, namely disease free and endemic equilibrium. For both disease free and endemic equilibrium, local and global stability is obtained here. Our disease-free equilibrium is locally asymptotically stable whenever R_0 is less than one, whereas the endemic equilibrium is locally asymptotically stable whenever R_0 is greater than one. Furthermore, the global stability of disease-free equilibrium has been proven by using Lyapunov function and the global stability of endemic equilibrium has been obtained by using Poincare Bendixson technique. Also, we enhance our analytic results by numerical simulation. At the end we have attempted to fit our proposed model with the real-world data.

Keywords: COVID-19; equilibria; basic reproduction number; local stability; global stability; numerical simulation.

2020 AMS Subject Classification: 92B05, 34H15, 34A34.

1. INTRODUCTION

A Mathematical model can be defined as the formulation of set of equations that express the essential features of a physical system or a process in mathematical terms. In other words, it is

*Corresponding author
E-mail address: gunasunc1@srmist.edu.in
Received November 15, 2022

actually a real-world problem that is converted into a mathematical term. There are four steps to construct and solve mathematical modelling. First, we understand the problem and describe it in mathematical terms, secondly, we will construct a basic model in which parameters and variables are defined logically. Thirdly, we will find different ways to solve the model. Finally, we will associate the solution or result of the proposed model to the real-world problem [1]. The main objective of mathematical modelling is to test the effect of changes in a system [2], [3]. In the modern global scenario, infectious disease investigation and control have received a lot of attention [4]. With increasing complications in human everyday life, as well as climatic change due to global warming, pathogens of numerous infectious diseases have become more active than in the past. As a result, in addition to medical diagnosis, a full theoretical examination of the related epidemic system is required. Mathematical models are very beneficial for describing an epidemic system in this theoretical inquiry [5], [6]. Kermack and Mckendric [7] were likely the first to accurately characterise an infectious disease system using a mathematical model. Also, many other researchers worked on mathematical modelling on the transmission of disease such as TB, dengue, HIV-AIDS, Nipah virus etc, which was described in [8], [9], [10], [11], [12], [13], [14]. Here we take COVID-19 as our real world problem and we try to frame a model logically which was described in section 2.

COVID-19 is a deadly infectious disease which was caused by a special type of coronavirus known as severe acute respiratory syndrome coronavirus 2, that was first emerged in December 2019 in the Large town of Wuhan [15]. The viral load is carried from person to person and has spread throughout China, followed by the rest of the world. The COVID-19 virus causes weak to moderate respiratory illness in the majority of persons who are infected with it, but they recover without needing any special treatment [16]. But older people and with low immunity are more likely to develop serious illness. Various safety measures such as social distancing, usage of medical masks and hand hygiene practices are recommended to prevent from the spread of the COVID-19, which was implemented immediately across the globe by the World Health organization. On March 12, 2020 World Health Organization declared the outbreak as pandemic [17]. There were only 1,18,000 cases in 114 countries at the time, with 4,291 individuals deceased. However, after that the number of cases increases rapidly and in a discontinuous manner. These

viruses attack the human population by different waves. Also, the rate of increase, both in the number of cases of infection, recovery and death, varies from region to region. Particularly in India, the first wave occurs between July to November 2020 followed by second wave between March to June 2021 and currently India is facing third wave of coronavirus. During first wave peak, India reported over 97,860 confirmed cases in September 2020 and during second wave peak, India reported 4,14,280 cases in May 2021 [18]. Till the end of 2020, India had lost over 1,51,364 peoples. So, to control the deaths and to gain immunity, the government of India had launched the vaccination drive from January 16, 2021 [19]. At early stage of vaccination drive, Indian people have lot of hesitancy. So, till the month of June 2021, India had administered 22,10,43,693 doses.

Recently, Fanelli and Piazza constructed a SIRD system by classifying the human population into four compartment as susceptible, infected, recovered and deceased classes. They modelled the continents of China, Italy and France using real data and predicted the transmission of COVID-19 in these countries [20]. J. Jiang et al. developed SEIR model to forecast the COVID-19 epidemic trends particularly in USA, New York and Italy [21]. The authors Quian li et al. [22] has proposed the impact of mass influenza vaccination model on COVID-19 epidemic. Here in our proposed work, we constructed SEIR Model by incorporating the fact of partially vaccinated and fully vaccinated individuals to the population. Then we analyse the behaviour of our model and also we studied their effects in some regions of India. Mainly we have focussed on four regions of India. We consider Tamil Nadu, Maharashtra, West Bengal and Delhi and studied their real data scenario of partially vaccinated and fully vaccinated population and tried to fit those data to our proposed model.

The following is an overview of our paper structure. The forthcoming section presents the four dimensional nonlinear mathematical model, followed by the boundedness and positivity. Section 3 provides an overview to equilibrium analysis and basic reproduction number. Section 4 deals with both local and global stability analysis of our proposed model. In section 5 we have presented our analytical solution in terms of numerical simulation and finally we have focussed on real data validation in section 6. The paper ends with brief conclusion in section 7.

2. THE MODEL FORMULATION

We consider the whole human population $N(t)$ and we have divided into four compartments namely Susceptible Individuals $S(t)$, Exposed Individuals $E(t)$, Infected Individuals $I(t)$ and Recovered Individuals $R(t)$. To build our system, the following assumptions has been made: Individuals are recruited in the region at a fixed rate A and joins the susceptible compartment. The susceptible population become exposed to the infection, when infected individual become contact at the rate α. Also we assume that, the exposed population become infected at a constant rate $\delta > 0$. Here we have incorporated partially vaccinated population V_p and fully vaccinated population V_f into the model to make it more realistic. So those who are partially vaccinated may get exposed and the fully vaccinated individuals directly moves to recovery compartment. Other than vaccinated individuals, the remaining infected individuals are recovered due to treatment at the rate γ.

So, by considering the above divisions and assumptions a simple nonlinear mathematical model is formulated.

$$\begin{aligned}
\frac{dS}{dt} &= A - \alpha SI - \mu S - V_p S - V_f S, \\
\frac{dE}{dt} &= \alpha SI - \mu E - \delta E + V_p S, \\
\frac{dI}{dt} &= \delta E - \mu I - \mu_1 I - \gamma I, \\
\frac{dR}{dt} &= V_f S + \gamma I - \mu R.
\end{aligned} \tag{1}$$

Further the model (1) is simplified as below:

$$\begin{aligned}
\frac{dS}{dt} &= A - \alpha SI - k_1 S, \\
\frac{dE}{dt} &= \alpha SI + V_p S - k_2 E, \\
\frac{dI}{dt} &= \delta E - k_3 I, \\
\frac{dR}{dt} &= V_f S + \gamma I - \mu R.
\end{aligned} \tag{2}$$

where,

$k_1 = \mu + V_p + V_f$,

$k_2 = \mu + \delta$ and

$k_3 = \mu + \mu_1 + \gamma$.

Parameters description of the model (1) is given in the Table 1. Also the transfer diagram of our model is described in Figure 1.

TABLE 1. Description of Parameters

Parameter	**Description**
A	Recruitment rate.
α	Rate of interaction between susceptible and infected individuals.
μ	Natural death rate.
V_p	Partially vaccinated population.
V_f	Fully vaccinated population.
δ	Exposed population becomes infected population at a constant rate $\delta > 0$.
μ_1	Disease related death.
γ	Rate of medication to recovery.

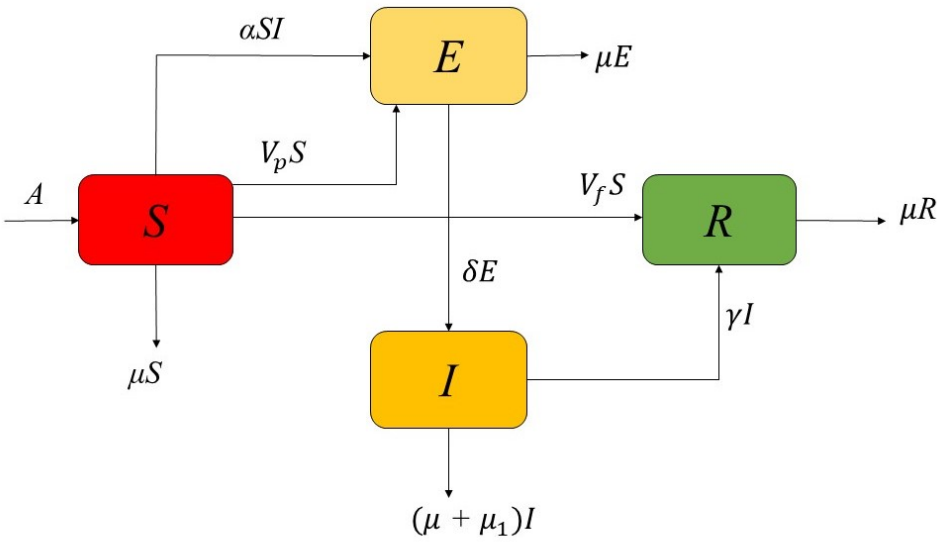

FIGURE 1. Transfer Diagram of the model (1).

2.1 Positivity and Boundedness of the model

In this subsection, we proved the positivity and boundedness of the system. From (1), we have

$\frac{dS}{dt}|_{S=0} = A > 0,$

$\frac{dE}{dt}|_{E=0} = \alpha SI + V_p S \geq 0,$

$\frac{dI}{dt}|_{I=0} = \delta E \geq 0,$

$\frac{dR}{dt}|_{R=0} = V_f S + \gamma I \geq 0.$

Clearly, all the population and parameters are non-negative in the region. Further from the model (1), the total population is $N = S+E+I+R$ and the rate of change of the total population is given by,

$$\frac{dN}{dt} = \frac{dS}{dt} + \frac{dE}{dt} + \frac{dI}{dt} + \frac{dR}{dt} = A - \mu N - \mu_1 I. \tag{3}$$

In absence of disease we have $I = 0$, therefore $\frac{dN}{dt} = A - \mu N$. This gives that lim sup $N \leq \frac{A}{\mu}$. Therefore all the solutions of S, E, I and R are bounded by $\frac{A}{\mu}$. Hence the biologically feasible region of the model (1) is provided by positive invariant set:

$$\xi = \left\{ (S,E,I,R) \in R^4 | S(t) \geq 0, E(t) \geq 0, I(t) \geq 0, R(t) \geq 0, S+E+I+R \leq \frac{A}{\mu} \right\}. \tag{4}$$

3. Equilibrium Analysis of the Model

In this, we analyse the existence of equilibrium points for the system (2). Here we obtained two equilibrium points namely E_0= (S^0, E^0, I^0, R^0) and E_1 = (S^*, E^*, I^*, R^*).

3.1 Disease Free Equilibrium Points (E_0)

For the proposed system, we obtained disease free equilibrium points $E_0 = \left(\frac{A}{k_1}, 0, 0, \frac{V_f A}{\mu k_1}\right)$.

3.2 Basic Reproduction Number (R_0)

The estimated number of secondary infections developed in susceptible individuals by a typical infected individual during his or her whole infectious period is denoted as the basic reproduction number. The reproduction number R_0 for the model is found out using the next generation matrix method which was mentioned in [23]. For this we consider, $\mathscr{F}(t)$, $\mathscr{V}^+(t)$ and $\mathscr{V}^-(t)$. Where $\mathscr{F}(t)$ is the rate at which new infections appear in the compartment, $\mathscr{V}^+(t)$ is the rate at which individuals are transferred into the compartment and $\mathscr{V}^-(t)$ is the rate at

which individuals are transferred out of the compartment. In this way, $\mathscr{F}(t)$, $\mathscr{V}^+(t)$ and $\mathscr{V}^-(t)$ are associated with the system (2). Which are obtained as,

$$\mathscr{F}(t) = \begin{pmatrix} \alpha SI \\ 0 \end{pmatrix}, \ \mathscr{V}^+(t) = \begin{pmatrix} V_p S \\ \delta E \end{pmatrix} \ and \ \mathscr{V}^-(t) = \begin{pmatrix} k_2 E \\ k_3 I \end{pmatrix}.$$

Considering, $\mathscr{V}(t)$ = $\mathscr{V}^-(t)$ - $\mathscr{V}^+(t)$. We get,

$$\mathscr{V}(t) = \begin{pmatrix} k_2 E - V_p S \\ k_3 I - \delta E \end{pmatrix}$$

$$\Rightarrow \mathscr{F}(t) - \mathscr{V}(t) = \left[\tfrac{dE}{dT}, \tfrac{dI}{dt}\right]^T$$

The Jacobian of $\mathscr{F}(t)$ and $\mathscr{V}(t)$ is obtained by F = Jacobian of $\mathscr{F}(t)$ at E_0 and V = Jacobian of $\mathscr{V}(t)$ at E_0.

$$\text{F} = \begin{pmatrix} 0 & \frac{A\alpha}{k_1} \\ 0 & 0 \end{pmatrix} \text{ and V} = \begin{pmatrix} k_2 & 0 \\ -\delta & k_3 \end{pmatrix}$$

Next, inverse of V is found by $\frac{Adj\text{V}}{|\text{V}|}$

$$\Rightarrow \text{V}^{-1} = \begin{pmatrix} \frac{1}{k_2} & 0 \\ \frac{\delta}{k_1 k_2 k_3} & \frac{1}{k_3} \end{pmatrix}$$

At last, the matrix FV^{-1} is given by,

$$\Rightarrow \text{FV}^{-1} = \begin{pmatrix} \frac{A\alpha\delta}{k_1 k_2 k_3} & \frac{A\alpha}{k_1 k_3} \\ 0 & 0 \end{pmatrix} \tag{5}$$

Thus the basic reproduction number of the system (2) is obtained by the dominant eigen value of FV^{-1}. Here, we obtain $R_0 = \frac{A\alpha\delta}{k_1 k_2 k_3}$.

3.3 Endemic Equilibrium Points (E_1)

For the proposed system, we obtained the endemic equilibrium points $E_1 = (S^*, E^*, I^*, R^*)$. where,

$S^* = \frac{k_2 k_3 I^*}{\delta(\alpha I^* + V_p)}$,

$E^* = \frac{k_3 I^*}{\delta}$,

$R^* = \frac{1}{\mu}\ [\frac{V_f k_2 k_3 I^*}{\delta(\alpha I^* + V_p)} + \gamma I^*]$,

I^* is the root of the following quadratic equation.

$$g(I^*) = M_1 I^{*2} + M_2 I^* + M_3 = 0, \tag{6}$$

TABLE 2. Existence of positive roots when $R_0 > 1$

Coefficients	Signs of coefficients	No of sign change	No of possible positive roots
M_1	$+$	0	No root
M_2	$-$	1	Unique root
M_3	$-$	0	No root

where,

$M_1 = k_2k_3\alpha$,

$M_2 = k_1k_2k_3 - A\delta\alpha$,

$M_3 = -A\delta V_p$.

Clearly, $M_1 > 0$, $M_3 < 0$ and $M_2 < 0$ when $R_0 > 1$. By using Descartes rule of signs, we get $g_1(I^*) = M_1I^{*2} - M_2I^* - M_3 = 0$. Therefore, unique positive endemic equilibrium root exists. So obviously the other root is negative. So we neglect the negative root.

4. STABILITY ANALYSIS

In this section we find both local and global stability of disease-free equilibrium and endemic equilibrium points. The Jacobi matrix for the model (2) is given by,

$$J = \begin{pmatrix} -\alpha I - k_1 & 0 & -\alpha S & 0 \\ \alpha I + V_p & -k_2 & \alpha S & 0 \\ 0 & \delta & -k_3 & 0 \\ V_f & 0 & \gamma & -\mu \end{pmatrix} \tag{7}$$

4.1 Local Stability Analysis

Disease Free Equilibrium (DFE)

Theorem 1

If $R_0 < 1$, E_0 is locally asymptotically stable and otherwise it is unstable.

Proof:

From model (2), the Jacobi matrix at disease free equilibrium $E_0 = (S^0, E^0, I^0, R^0) =$

$\left(\frac{A}{k_1}, 0, 0, \frac{V_f A}{\mu k_1}\right)$ is obtained as follows,

$$J_0 = \begin{pmatrix} -k_1 & 0 & \frac{-\alpha A}{k_1} & 0 \\ V_p & -k_2 & \frac{\alpha A}{k_1} & 0 \\ 0 & \delta & -k_3 & 0 \\ V_f & 0 & \gamma & -\mu \end{pmatrix} \tag{8}$$

Clearly, $-\mu$ is one of the eigen value of J_0 matrix. The other three eigen value are computed from the below matrix.

$$A_0 = \begin{pmatrix} a_{11} & a_{12} & a_{13} \\ a_{21} & a_{22} & a_{23} \\ a_{31} & a_{32} & a_{33} \end{pmatrix}$$

where,

$a_{11} = -k_1, \;\; a_{21} = V_p, \;\; a_{31} = 0,$

$a_{12} = 0, \qquad a_{22} = -k_2, \; a_{32} = \delta,$

$a_{13} = \frac{-\alpha A}{k_1}, \; a_{23} = \frac{\alpha A}{k_1}, \;\; a_{33} = -k_3.$

The characteristic equation corresponding to matrix A_0 is obtained from,

$$\Lambda^3 + a_1\Lambda^2 + a_2\Lambda + a_3 = 0 \tag{9}$$

where,

$a_1 = -[a_{11} + a_{22} + a_{33}],$

$a_2 = a_{22}a_{33} - a_{32}a_{23} + a_{11}a_{33} - a_{31}a_{13} + a_{11}a_{22} - a_{21}a_{12},$

$a_3 = -|A_0|.$

According to Routh Hurwitz Criteria disease free equilibrium, E_0 is locally asymptotically stable if it satisfies $a_1 > 0$, $a_3 > 0$ and $a_1 a_2 > a_3$. Here we get $a_1 = k_1 + k_2 + k_3$, $a_2 = k_2k_3 + k_1k_3 + k_1k_2 - \frac{\alpha A\delta}{k_1}$, $a_3 = k_1k_2k_3 + \frac{\alpha A V_p \delta}{k_1} - \alpha A\delta$.

So from above clearly we can say, $a_1 > 0$, $a_2 > 0$ when $R_0 < 1$ if and only if $k_2k_3 - \frac{A\alpha\delta}{k_1} > 0$ and $a_3 > 0$ when $R_0 < 1$ if and only if $k_1k_2k_3 - A\alpha\delta > 0$.

Hence disease free equilibrium $E_0 = (S^0, E^0, I^0, R^0)$ is locally asymptotically stable whenever

$R_0 < 1$. This completes the proof.

Endemic Equilibrium (EE)

Theorem 2

If $R_0 > 1$, E_1 is locally asymptotically stable and otherwise it is unstable.

Proof:

From model (2), the Jacobi matrix at endemic equilibrium $E_1 = (S^*, E^*, I^*, R^*)$ is obtained as follows,

$$J_1 = \begin{pmatrix} -\alpha I^* - k_1 & 0 & -\alpha S^* & 0 \\ \alpha I^* + V_p & -k_2 & \alpha S^* & 0 \\ 0 & \delta & -k_3 & 0 \\ V_f & 0 & \gamma & -\mu \end{pmatrix} \tag{10}$$

Clearly, $-\mu$ is one of the eigen value of J_1 matrix. The other three eigen value are computed from the below matrix.

$$B_1 = \begin{pmatrix} b_{11} & b_{12} & b_{13} \\ b_{21} & b_{22} & b_{23} \\ b_{31} & b_{32} & b_{33} \end{pmatrix}$$

where,

$b_{11} = -\alpha I^* - k_1, \quad b_{21} = \alpha I^* + V_p, \quad b_{31} = 0,$

$b_{12} = 0, \qquad b_{22} = -k_2, \qquad b_{32} = \delta,$

$b_{13} = -\alpha S^*, \qquad b_{23} = \alpha S^*, \qquad b_{33} = -k_3.$

The characteristic equation corresponding to matrix B_1 is obtained from,

$$\Lambda^3 + b_1\Lambda^2 + b_2\Lambda + b_3 = 0 \tag{11}$$

where,

$b_1 = \alpha I^* + k_1 + k_2 + k_3,$

$b_2 = \alpha k_2 I^* + \alpha k_3 I^* + k_1 k_3 + k_1 k_2 + k_2 k_3 - \alpha\delta S^*,$

$b_3 = \alpha k_2 k_3 I^* + \alpha\delta V_p S^* + k_1 k_2 k_3 - \alpha\delta k_1 S^*.$

Now, according to Routh Hurwitz Criteria endemic equilibrium, E_1 is locally asymptotically

stable if it satisfies $b_1 > 0$, $b_3 > 0$ and $b_1 b_2 > b_3$. Here clearly, $b_1 > 0$, $b_2 > 0$ when R_0 is greater than one, if and only if $k_2 k_3 - S^* \alpha\delta < 0$ and $b_3 > 0$ when R_0 is greater than one, if and only if $k_1 k_2 k_3 - \alpha\delta k_1 S^* < 0$.

Hence endemic equilibrium $E_1 = (S^*, E^*, I^*, R^*)$ is locally asymptotically stable whenever R_0 is greater than one. This completes the proof.

4.2 Global Stability Analysis

Disease Free Equilibrium (DFE)

Theorem 3

If $R_0 < 1$, Disease free equilibrium of system (2) is globally asymptotically stable and unstable otherwise.

Proof:

The Lyapunov function for our proof is constructed as follows,

$$V_1 = k_3 I + mR \text{ for every } m \geq 0. \tag{12}$$

Now, differentiating with respect to time we get,

$$\dot{V_1} = k_3 \dot{I} + m\dot{R}$$

$$\dot{V_1} = k_3(\delta E - k_3 I) + m(V_f S + \gamma I - \mu R)$$

Since we know, $S \leq 0$, $E \leq 0$ and $R \leq \frac{V_f A}{\mu k_1}$. So, we replace and proceed as,

$$\dot{V_1} \leq [-k_3^2 + R_0] I, \tag{13}$$

where $R_0 = \frac{A\alpha\delta}{k_1 k_2 k_3}$

Clearly, for $I = 0$, we get $\dot{V_1} = 0$ and $\dot{V_1} \leq 0$ if and only if $R_0 < 1$. It follows from Lasalle's Invariance Principle, that is every solution to the system (2) with initial condition in ξ approaches disease free equilibrium as t $\to \infty$. Since we already know region ξ is positively invariant, which was described in (4).

Therefore E_0 is globally asymptotically stable in the region ξ whenever R_0 is less than one.

Hence the proof.

Endemic Equilibrium (EE)

In this subsection, the global stability of endemic equilibrium is derived with the help of Poincare Bendixson technique. Let $g(x) : H \subset R^n \to R^n$ be a map, where H is an open set and if $E^{'} = g(x)$ be a differential equation, then by using the initial condition $x(t)= x_0$, the solution can be determined.

- H is simply connected.
- There exists a compact absorbing subset K of H.
- In H, $\bar{x}$ is the globally stable equilibrium point whenever

$$\dot{q_2} = \lim_{t\to\infty} \sup \sup_{x_0\in k} q < 0$$

where $q = \int_0^t \Psi(W)dt$. Here W is constructed as $\mathscr{P}_f \mathscr{P}^{-1} + \mathscr{P} J_2^{|2|} \mathscr{P}^{-1}$, where $\mathscr{P}$ be the matrix satisfies $\Psi(\mathscr{P}_f \mathscr{P}^{-1} + \mathscr{P} J_2^{|2|} \mathscr{P}^{-1}) \leq 0$, where $J_2^{|2|} = \frac{\partial g^{|2|}}{\partial x}$ is the second additive compound Jacobian matrix of order two and Ψ denotes the Lozinskii measure [24].

Theorem 4

The system is globally asymptotically stable in the region ξ, whenever R_0 is greater than one.

Proof:

Leaving the recovered population, the Jacobi matrix can be written as,

$$J_2 = \begin{pmatrix} -\alpha I - k_1 & 0 & -\alpha S \\ \alpha I + V_p & -k_2 & \alpha S \\ 0 & \delta & -k_3 \end{pmatrix} \tag{14}$$

Also we know that, for $A_1 = (a_{ij})$,

$$A_1^{|2|} = \begin{pmatrix} a_{11} + a_{22} & a_{23} & -a_{13} \\ a_{32} & a_{11} + a_{33} & a_{12} \\ -a_{31} & a_{21} & a_{22} + a_{33} \end{pmatrix}$$

And hence the second additive compound matrix $(J_2^{|2|})$ is obtained as,

$$J_2^{|2|} = \begin{pmatrix} -\alpha - k_1 - k_2 & \alpha S & \alpha S \\ \delta & -\alpha I - k_1 - k_3 & 0 \\ 0 & \alpha I + V_p & -k_2 - k_3 \end{pmatrix}$$

To find the matrix W, we define a diagonal matrix $\mathscr{P}$ = diag $\{1, \frac{E}{I}, \frac{E}{I}\}$.

Let f be the vector field of the model, then $\mathscr{P}_f\ \mathscr{P}^{-1}$ = diag $\left\{0, \frac{E^{'}}{E} - \frac{I^{'}}{I}, \frac{E^{'}}{E} - \frac{I^{'}}{I}\right\}$.

Hence W matrix is given by,

$$W = \mathscr{P}_f \mathscr{P}^{-1} + \mathscr{P} J_2^{|2|} \mathscr{P}^{-1} = \begin{pmatrix} w_{11} & w_{12} \\ w_{21} & w_{22} \end{pmatrix} \tag{15}$$

$$W = \begin{pmatrix} -\alpha - k_1 - k_2 & \alpha S\frac{I}{E} & \alpha S\frac{I}{E} \\ \frac{E}{I}\delta & -\alpha I - k_1 - k_3 + Y & 0 \\ 0 & \alpha I + V_p & -k_2 - k_3 + Y \end{pmatrix}$$

where, $Y = \frac{E^{'}}{E} - \frac{I^{'}}{I}$.

Therefore, block matrix can be written as,

$$W = \begin{pmatrix} w_{11} & w_{12} \\ w_{21} & w_{22} \end{pmatrix},$$

$$w_{11} = \left(-\alpha - k_1 - k_2\right),$$

$$w_{12} = \begin{pmatrix} \alpha S\frac{I}{E} & \alpha S\frac{I}{E} \end{pmatrix},$$

$$w_{21} = \begin{pmatrix} \frac{E}{I}\delta \\ 0 \end{pmatrix},$$

$$w_{22} = \begin{pmatrix} -\alpha I - k_1 - k_3 + Y & 0 \\ \alpha I + V_p & -k_2 - k_3 + Y \end{pmatrix}.$$

Now, the Lozinskii measure of W is obtained from $\Psi(W) \leq$ Sup $\{g_1\ ,\ g_2\}$, where $g_1 = \Psi(w_{11}) + |w_{12}|$ and $g_2 = |w_{21}| + \Psi(w_{22})$.

Hence,

$$g_1 = -\alpha I - k_1 - k_2 + \frac{\alpha SI}{E},$$
$$g_2 = Y - k_3 - k_1 + V_p + \frac{\delta E}{I}.$$

Now from model (2), the equation is rewritten as,

$$\frac{\alpha SI}{E} = \frac{E^{'}}{E} + k_2 - \frac{V_p S}{E},$$
$$\frac{\delta E}{I} = \frac{I^{'}}{I} + k_3.$$

By substituting in g_1 and g_2 we get,

$$g_1 \leq \frac{E^{'}}{E} - \mu,$$
$$g_2 \leq \frac{E^{'}}{E} - \mu.$$
$$\Rightarrow \Psi(W) \leq \frac{E^{'}}{E} - \mu.$$

Hence $\int_0^t \Psi(W)dt < logE(t) - \mu(t)$ and so $\dot{q_2} = \frac{\int_0^t \Psi(W)dt}{t} < \frac{logE(t)}{t} - \mu < 0$ for all $(S(0), E(0),$ $I(0),$ $R(0))$ in the absorbing set. Therefore $\dot{q_2}$ is strictly less than zero, which satisfies the condition. Therefore, the endemic equilibrium is globally stable in the region ξ. Hence the proof.

5. NUMERICAL SIMULATION

In this section, we simulate the proposed model (1) by assuming different set of parameters. We consider the following set. $A = 17000$, $\alpha = 0.0006$, $\delta = 0.0079$, $\gamma = 0.0929$, $\mu = 0.989$, $\mu_1 = 0.1$, $R_0 = 0.969$, $V_p = 0.0001$ and $V_f = 0.03$. For the above set we obtained R_0 as 0.0159, which is less than one. Therefore, disease free equilibrium is stable. This fact is illustrated in Figure 2 (a). Next, we make some changes in parameter which corresponds to endemic equilibrium. For this case we obtained R_0 as greater than one. Therefore, endemic equilibrium is stable. Which is also illustrated in Figure 2 (b).

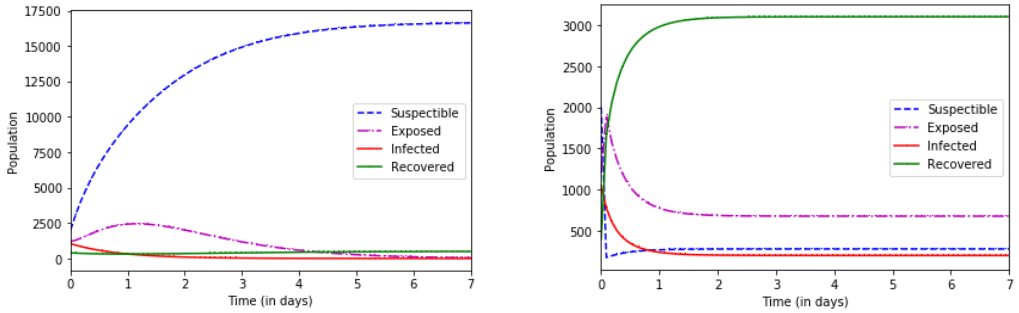

FIGURE 2. (a) Disease free equilibrium of model (2) and (b) Endemic equilibrium of model (2).

Now, for the *SEIR* system (1) we prove the results numerically with the help of python. The parameter values have been chosen as, $\alpha = 0.0006$, $\delta = 0.0079$, $\gamma = 0.0929$, $\mu = 0.989$ and $\mu_1 = 0.1$. Figure 3 (a) shows the time plot of system (1) for the disease free equilibrium in the absence of V_p and V_f with the following set of parameters, $V_p = 0$, $V_f = 0$. The value of R_0 is obtained as 0.0959 which is less than one. Also from the Figure 3 (a), we can clearly note that the infection will vanish out in a short period of time. Figure 3 (b) demonstrates the effect of partially vaccinated individuals on the exposed population. This clearly indicates that the exposed population increases gradually whenever we increase the parameter V_p as 0.1, 0.2, 0.3 and 0.4 respectively.

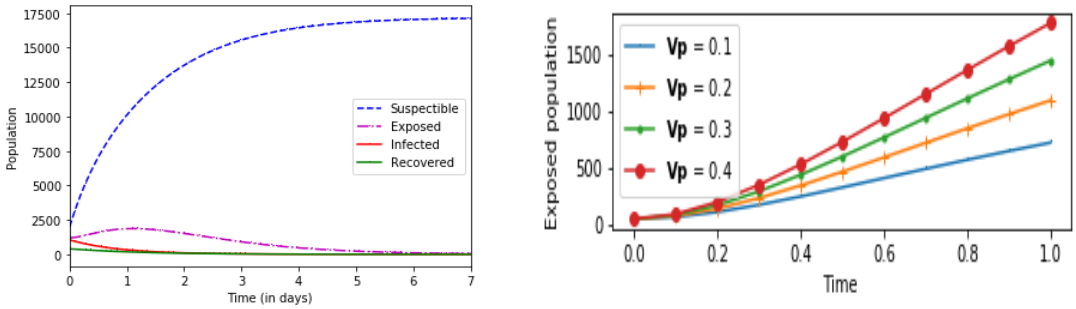

FIGURE 3. (a) Local stability of V_p and V_f when $R_0 < 1$ and (b) Effect of V_p on exposed population.

Figure 4 (a), (b) and (c) demonstrates the effect of fully vaccinated individuals on the recovered population. It clearly shows that recovered population increases gradually whenever we increase the parameter V_f by 0.3, 0.6 and 1 respectively.

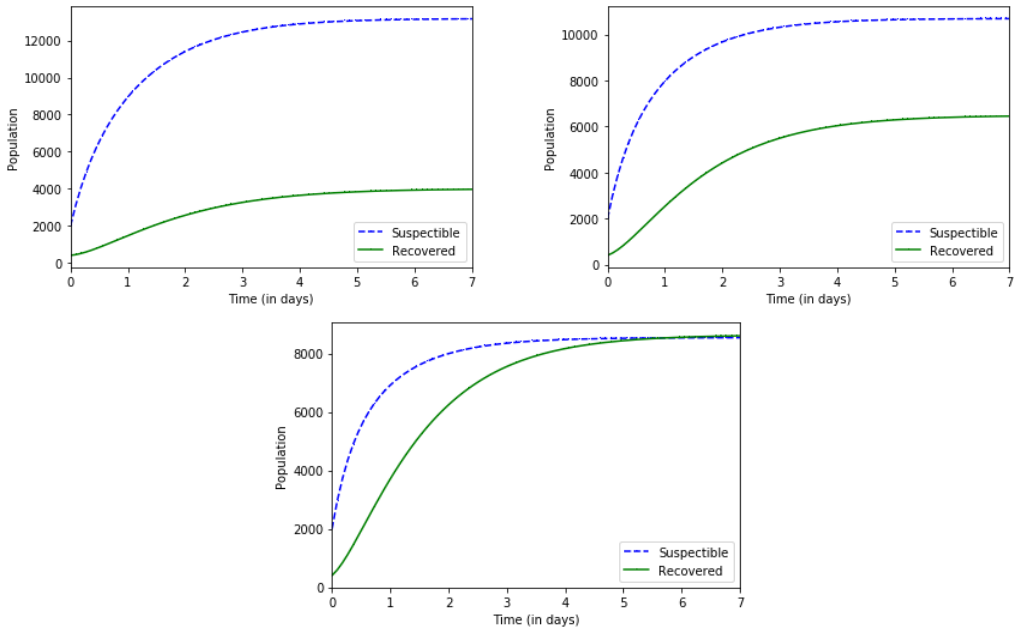

FIGURE 4. (a) Effect of V_f on recovered population, when $V_f = 0.3$, (b) Effect of V_f on recovered population, when $V_f = 0.6$ and (c) Effect of V_f on recovered population, when $V_f = 1$

Figure 5 demonstrates the effect of both fully and partially vaccinated individuals. First, we consider 5% of population are fully vaccinated and 15% are partially vaccinated from the total assumed population. From 5 (a) we interpret that 5% of V_f and 15% of V_p to the population, gradually increases the recovered population and gradually decreases the exposed population. Also, the value of R_0 is obtained as 4.765. Whereas in Figure 5 (b), we consider 60% are fully vaccinated and 30% are partially vaccinated individuals. From this we interpret that 60% of V_f and 30% of V_p to the population, drastically increases the recovered population and drastically decreases the exposed population. Also, the value of R_0 is obtained as 1.059, which is closer to one. In another way, we can say that increase in parameter V_f decreases the basic reproduction number R_0.

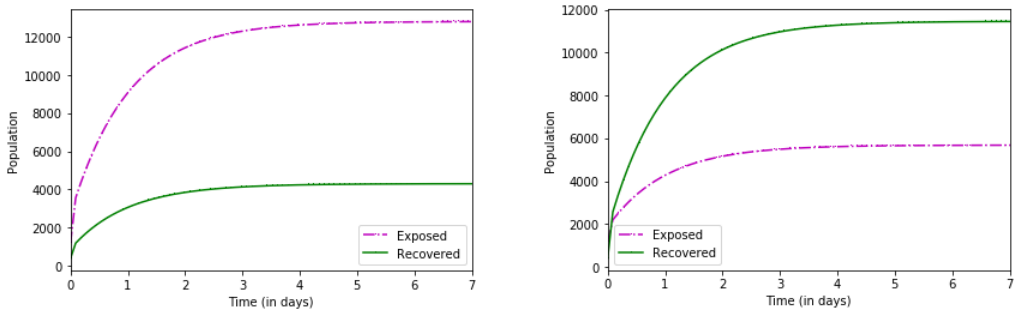

FIGURE 5. (a) Effect of both V_p and V_f, when $V_p = 15\%$ and $V_f = 5\%$ and (b) Effect of both V_p and V_f, when $V_p = 30\%$ and $V_f = 60\%$.

6. REAL DATA VALIDATION

As reported by covid19bharat.org, India has 4,17,95,478 confirmed cases till February 03, 2022, whereas the popular and developed regions like Tamil Nadu, Maharashtra, West Bengal and Delhi has 33,75,329, 77,53,548, 20,00,253 and 18,35,979 cases respectively. So continuously COVID-19 confirmed cases has booms and depressions in a short span of two years. Now, currently India is facing third wave of pandemic. To control and to prevent each one, the government of India had launched vaccination drive from January 16th, 2021.

Till first week of February, India had administrated 167,85,72,152 doses to the eligible population. In that 94,67,21,905 individuals had taken first dose, whereas 71,89,78,491 individuals had completed their second dose i.e., 70.8% of the population are partially vaccinated and 53.7% have been fully vaccinated. Here we are concentrating on partially and fully vaccinated data of India to fine tune the model (1). For our case, we consider four regions from India namely Tamil Nadu, Maharashtra, West Bengal and Delhi. From these four regions we have collected partially and fully vaccinated population data, which was described in Table 3. A total of twelve months between January 16, 2021 and December 31, 2021 real data has been collected from https://www.cowin.gov.in.

TABLE 3. Real data on V_p and V_f from January 16 to December 31, 2021

Regions	Months	Partially vaccinated individuals	Fully vaccinated individuals
Tamil Nadu	Jan to Jun	13020552	2625266
	Jul to Dec	23139008	30132860
Maharashtra	Jan to Jun	25402887	6588439
	Jul to Dec	52299317	46716369
West Bengal	Jan to Jun	16484930	5462391
	Jul to Dec	47088855	34736096
Delhi	Jan to Jun	5698429	1868398
	Jul to Dec	9402651	9273997

TABLE 4. System parameters used for V_p data fitting

Parameters	Tamil Nadu	Maharashtra	West Bengal	Delhi
A	5600000	9200000	5200000	1500000
α	0.0002	0.0005	0.0005	0.0069
δ	0.0210	0.0210	0.0210	0.0210
γ	0.0999	0.999	0.999	0.099
μ	0.989	0.989	0.989	0.2987
μ_1	0.8	0.999	0.811	0.999
V_p	1.0001	3.0001	3.1102	0.0012
V_f	0.03	0.003	0.0003	0.03

From the above data, we can see the more number of doses administrated in West Bengal and less number administrated in Delhi. Also, we make some reasonable assumptions to the parameter, which was described in Table 4 and Table 5. By using python software, we tried to fit the simulated and observed data from all the considered regions during the time period from January 2021 to December 2021. Figure 6 demonstrates the real scenario of partially vaccinated and fully vaccinated individuals of the regions of Tamil Nadu, Maharashtra, West Bengal and Delhi for the time period of twelve months.

TABLE 5. System parameters used for V_f data fitting

Parameters	**Tamil Nadu**	**Maharashtra**	**West Bengal**	**Delhi**
A	900000	2200000	3800000	650000
α	0.0005	0.0005	0.0005	0.0080
δ	0.0210	0.0210	0.0210	0.0210
γ	1.0999	1.0999	1.0999	0.099
μ	0.3989	0.989	0.989	0.989
μ_1	0.9	0.8	0.9108	0.99999
V_p	1.0001	3.0001	3.1102	0.0012
V_f	0.03	0.003	0.0003	0.03

In Figure 7, we tried to fit the monthly cumulative partially and fully vaccinated data of four regions. In that blue dots represents the observed vaccinated data and the red curve represents the corresponding fitted curve from our proposed model (1). Figure 7 (a) demonstrates that, the fitted curve and observed data of partially vaccinated population of Tamil Nadu are very much nearest to each other except August, September and November months and in the case of fully vaccinated population the fitted curve and observed data are very close to each other till the month of August. After August, the real data increases drastically. Similarly in 7 (b), both fitted curve and observed data of partially vaccinated population of Maharashtra are close to each other except August and September and in the fully vaccinated case, the real data increases drastically after the month of July.

Figure 7 (c) demonstrates the data fitting of partially and fully vaccinated data of West Bengal. In West Bengal the simulated data and real data are very close to each other except October, since this was the only region who have administrated more number of first doses to the population in the month of October. So, the real data shows more variation. Also, this was the only region who have administrated more number of second doses in December month. So, in that month, the real data shows more deviation in fully vaccinated data fitting of West Bengal. Similarly figure 7 (d) shows the data fitting of Delhi, which also shows the simulated results are close to real data.

Overall, from the graphs, we observe that in the regions of Tamil Nadu, Maharashtra and Delhi, the fully vaccinated population real data increases drastically. That is administration of V_f to the population increases, whereas in West Bengal the fully vaccinated data increases from the month of November. So, at the beginning the vaccination drive in all the considered region was slow but at the second half of the year, especially from the month of August it increases gradually. Mainly administration of V_f to the population increases drastically.

So, from the proposed model we can comment that, increase in V_f increases the recovered population. So that completely vaccinated individuals will have less impact to the infection and moves directly to the recovered class. Due to sudden jump in vaccination drive, we predict that the infected people from virus decreases. So that the infection due to virus may start decreasing in the forthcoming waves.

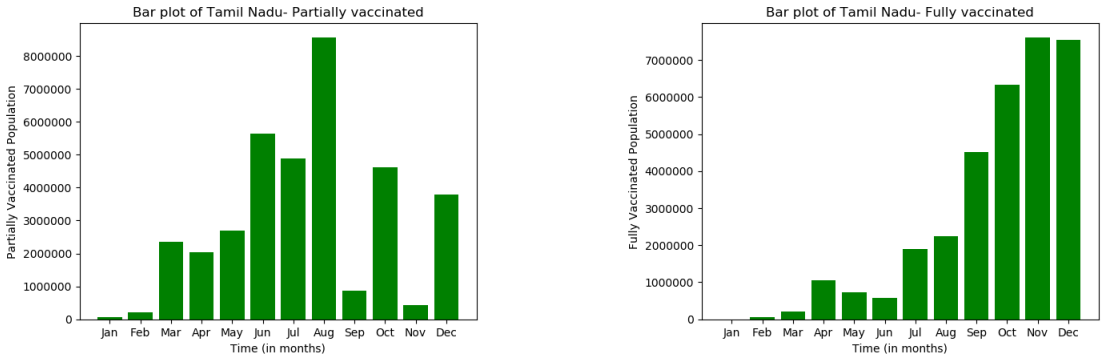

(a) Tamil Nadu

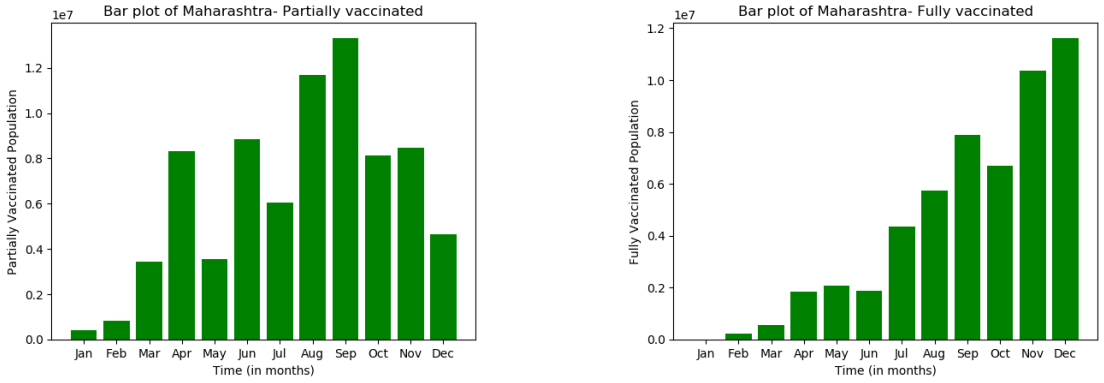

(b) Maharashtra

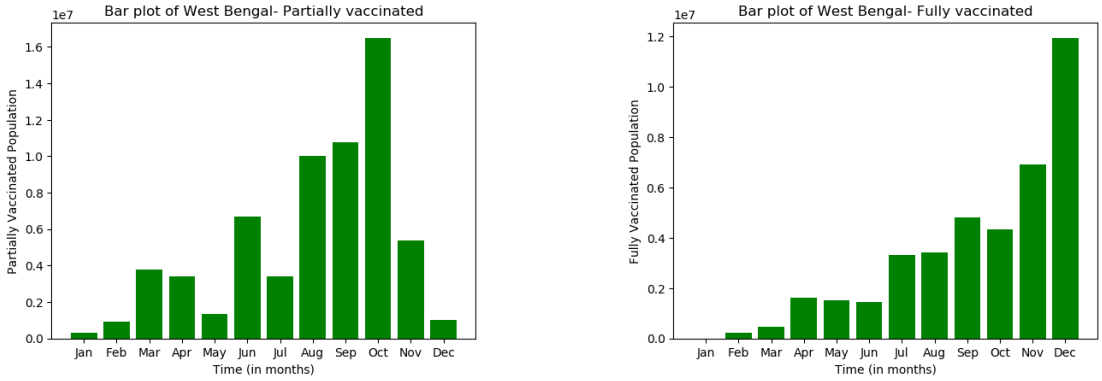

(c) West Bengal

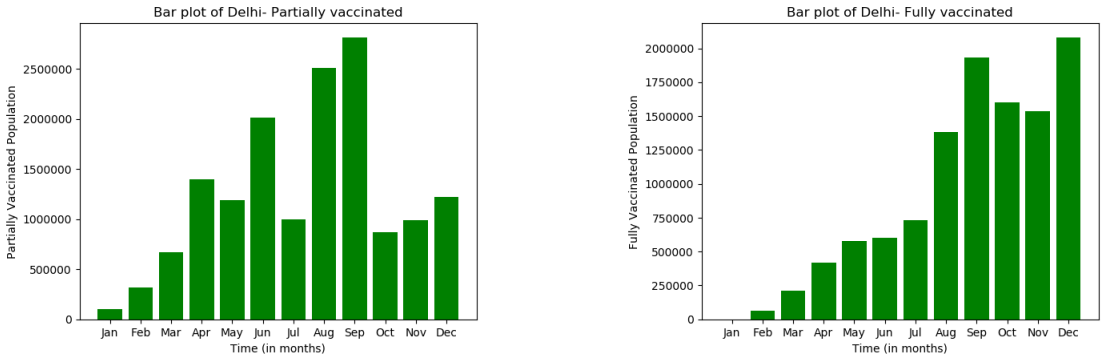

(d) Delhi

Figure 6: Monthly V_p and V_f real world data for different regions of India.

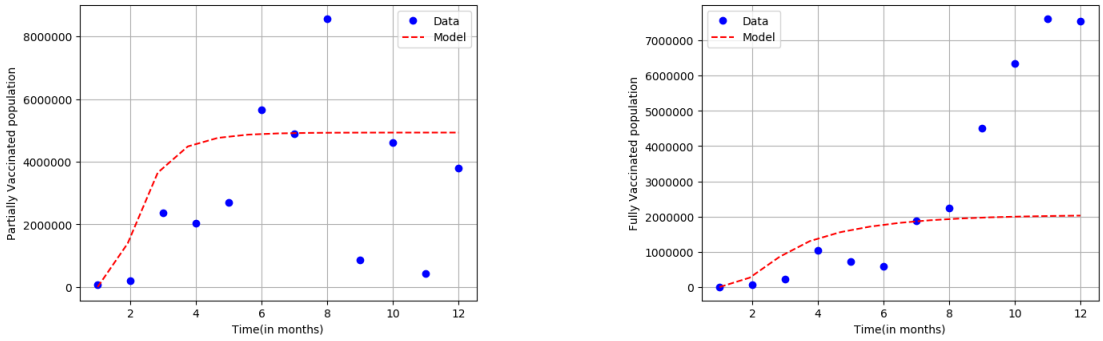

(a) Tamil Nadu

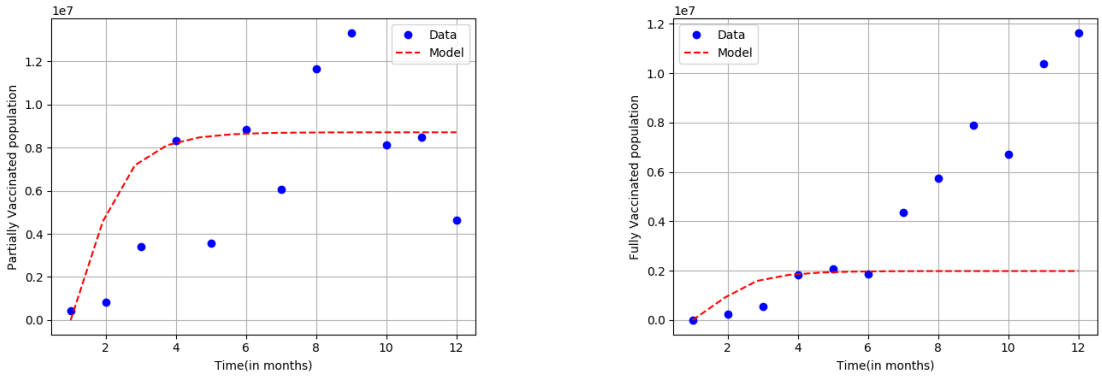

(b) Maharashtra

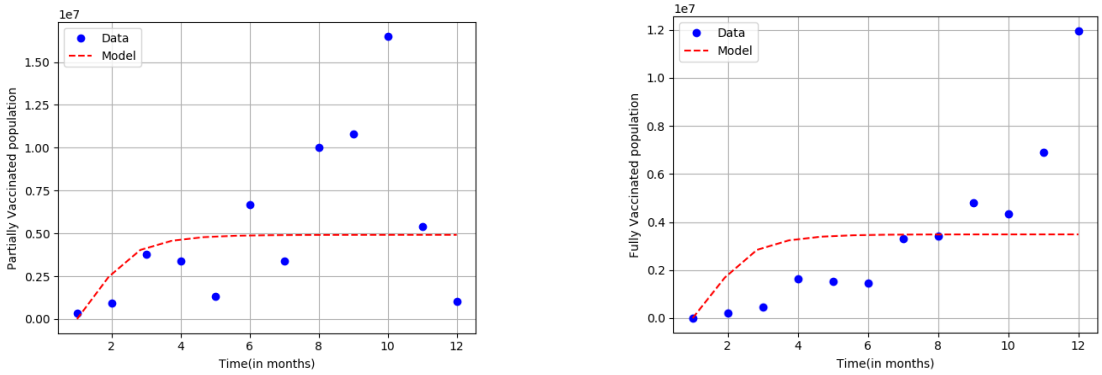

(c) West Bengal

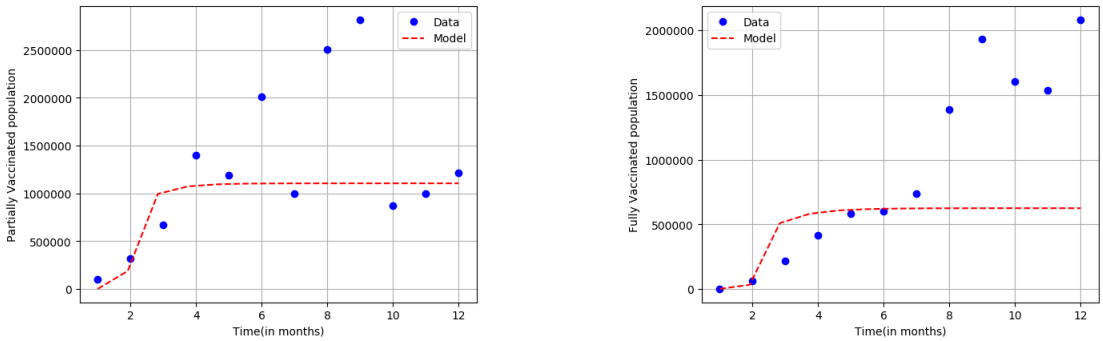

(d) Delhi

Figure 7: Plots of fitted model and the observed V_p and V_f data for different regions of India.

7. Conclusion

In this paper, a four-dimensional *SEIR* model of COVID-19 is developed and analysed with the effects of partially and fully vaccinated individuals in some regions of India. From our proposed model we find some of the mathematical findings, which was discussed here. Our model exhibits both disease free equilibrium and endemic equilibrium. Both are locally asymptotically stable whenever $R_0 < 1$ and $R_0 > 1$ respectively. Furthermore, Lyapunov function is constructed to show that, our disease-free equilibrium is globally asymptotically stable whenever $R_0 < 1$. Next, by using Poincare Bendixson technique we also proved that our endemic equilibrium is globally asymptotically stable in the region ξ, provided $R_0 > 1$. Then numerical simulation is performed for different set of parameters and from that we observed that, the exposed population is directly proportional to the partially vaccinated individuals and the recovered population is directly proportional to the fully vaccinated individuals. Finally, we validated our proposed model with the real-world data, which indicates that the infection due to virus may start decreasing in the forthcoming waves, since in all the studied regions, the fully vaccination drive has a sudden jump at the second half of the year 2021. So that from our model we comment that, infected people due to virus may decrease due to the increase in fully vaccination drive to the individuals particularly in the regions of Tamil Nadu, Maharashtra, West Bengal and Delhi.

Conflict of Interests

The author(s) declare that there is no conflict of interests.

References

[1] S.M. Moghadas, Majid Jaberi Douraki, Mathematical Modelling, A Graduate Textbook, John Wiley and Sons Inc. (2019).

[2] N.B. Sharmila, C. Gunasundari, Travelling wave solutions for a diffusive prey-predator model with one predator and two preys, Int. J. Appl. Math. 35 (2022), 661-684. https://doi.org/10.12732/ijam.v35i5.3.

[3] G. Santhosh Kumar, C. Gunasundari, Turing instability of a diffusive predator-prey model along with an Allee effect on a predator, Commun. Math. Biol. Neurosci. 2022 (2022), 40. https://doi.org/10.28919/cmbn/7361.

[4] M. Aakash, C. Gunasundari, Mathematical modeling and simulation of SEIR model for COVID-19 outbreak: A case study of trivandrum, Front. Appl. Math. Stat. 9 (2023), 1124897. https://doi.org/10.3389/fams.2023.1124897.

[5] M. Senthilkumaran, C. Gunasundari, Stability analysis of delayed prey-predator model with disease in the prey, Int. J. Comput. Appl. Math. 12 (2018), 356-377.

[6] G. Chandrasekar, S.M. Boulaaras, S. Murugaiah, A.J. Gnanaprakasam, B.B. Cherif, Analysis of a Predator-Prey Model with Distributed Delay, J. Funct. Spaces. 2021 (2021), 9954409. https://doi.org/10.1155/2021/9954409.

[7] W.O. Kermack, A.G. McKendrick, A contribution to the mathematical theory of epidemics, Proc. R. Soc. Lond. A. 115 (1927), 700–721. https://doi.org/10.1098/rspa.1927.0118.

[8] A.O. Egonmwan, D. Okuonghae, Analysis of a mathematical model for tuberculosis with diagnosis, J. Appl. Math. Comput. 59 (2018), 129–162. https://doi.org/10.1007/s12190-018-1172-1.

[9] A.S. Waziri, E.S. Massawe, O.D. Makinde, Mathematical modelling of HIV/AIDS dynamics with treatment and vertical transmission, Appl. Math. 2 (2012), 77–89. https://doi.org/10.5923/j.am.20120203.06.

[10] O. Diekmann, J.A.P. Heesterbeek, M.G. Roberts, The construction of next-generation matrices for compartmental epidemic models, J. R. Soc. Interface. 7 (2009), 873–885. https://doi.org/10.1098/rsif.2009.0386.

[11] A. Rusliza, H. Budin, Stability analysis of mutualism population model with time delay, Int. J. Math. Comput. Phys. Electric. Computer Eng. 6 (2012), 151-155.

[12] O.O. Apenteng, N.A. Ismail, Modelling the spread of HIV and AIDS epidemic trends in male and female populations, World J. Model. Simul. 13 (2017), 183-192.

[13] E. Demirci, A. Unal, N. Ozalp, A fractional order SEIR model with density dependent death rate, Hacettepe J. Math. Stat. 40 (2011), 287-295.

[14] S. Side, A susceptible-infected-recovered model and simulation for transmission of tuberculosis, Adv. Sci. Lett. 21 (2015), 137–139. https://doi.org/10.1166/asl.2015.5840.

[15] A. Susilo, C.M. Rumende, C.W. Pitoyo, et al. Coronavirus disease 2019: Tinjauan literatur terkini, Jurnal Penyakit Dalam Indonesia. 7 (2019), 45-67.

[16] B.K. Mishra, A.K. Keshri, Y.S. Rao, et al. COVID-19 created chaos across the globe: Three novel quarantine epidemic models, Chaos Solitons Fractals. 138 (2020), 109928. https://doi.org/10.1016/j.chaos.2020.109928.

[17] https://www.who.int/health-topics/coronavirus (accessed January 08, 2022).

[18] https://covid19.bharat.org (accessed January 08, 2022).

[19] https://www.mohfw.gov.in (accessed January 08, 2022).

[20] D. Fanelli, F. Piazza, Analysis and forecast of COVID-19 spreading in China, Italy and France, Chaos Solitons Fractals. 134 (2020), 109761. https://doi.org/10.1016/j.chaos.2020.109761.

[21] J. Jiang, L. Jiang, G. Li, et al. Prediction of the epidemic trends of COVID-19 by the improved dynamic SEIR model, (2020). https://doi.org/10.21203/rs.3.rs-28192/v1.

[22] Q. Li, B. Tang, N.L. Bragazzi, et al. Modeling the impact of mass influenza vaccination and public health interventions on COVID-19 epidemics with limited detection capability, Math. Biosci. 325 (2020), 108378. https://doi.org/10.1016/j.mbs.2020.108378.

[23] P. van den Driessche, J. Watmough, Reproduction numbers and sub-threshold endemic equilibria for compartmental models of disease transmission, Math. Biosci. 180 (2002), 29-48. https://doi.org/10.1016/s0025-5564(02)00108-6.

[24] M.Y. Li, J.S. Muldowney, A geometric approach to global-stability problems, SIAM J. Math. Anal. 27 (1996), 1070–1083. https://doi.org/10.1137/s0036141094266449.